Nanomaterials in Humans: Identification, Characteristics, and Potential Damage

Yuguo Song[1], **Xue Li**[2], **Liying Wang**[3], **Yon Rojanasakul**[4], **Vincent Castranova**[3], **Huiling Li**[1], and **Jing Ma**[1]

[1]Department of Occupational Medicine and Clinical Toxicology, Beijing Chaoyang Hospital, Capital University of Medical Sciences, Beijing, China

[2]Department of Pathology, Beijing Chaoyang Hospital, Capital University of Medical Sciences, Beijing, China

[3]Department of Pathology and Physiology, National Institute for Occupational Safety and Health, Morgantown, West Virginia, USA

[4]Department of Basic Pharmaceutical Sciences, West Virginia University, Morgantown, West Virginia, USA

Abstract

Nanomaterials are increasingly being used for commercial purposes. However, concerns about the potential risks of exposure to humans have been raised. We previously reported unusual pulmonary disease and death in a group of patients with occupational exposure to spray paint. However, the nanoparticle and chemical composition of the exposure was not fully described. The present study aimed to isolate and identify the nanoparticles observed in the patients' biopsies and report the potential deleterious effects to human lungs using electron microscopy. Using electron microscopy and energy dispersive x-ray analysis, silica nanoparticles were identified and characterized mainly in macrophages, pulmonary microvessels, vascular endothelial cells, microlymphatic vessels, pleural effusions, and a few in alveolar epithelial cells and pulmonary interstitial tissue (with no microscale particles present). Notably, damage to alveolar epithelial cells, macrophages, vascular endothelial cells, and the blood–gas barrier was observed. Given the well-documented toxicity of microscale silica, it is possible that these silica nanoparticles may have contributed in part to the illness reported in these workers. Such a possibility supports the adoption of controls and prevention strategies to minimize inhalation of nanoparticles by workers, and it highlights the urgent need and the importance of the nanosafety study in humans.

Keywords

human; pleural effusion; pulmonary fibrosis; silica nanoparticle

Nanotechnology has been regarded as a new technological revolution that touches almost every aspect of human life, making its presence felt in areas such as electronics, coatings, optical devices, energy, and medicine. It is estimated that the worldwide market for nanomaterials will grow to $3.1 trillion by 2015 (Lux report 2008). On the other hand, because of their widespread use, small size, large surface area, and metal contaminants, nanomaterials may exhibit unique bioactivity and interaction with cellular or subcellular structures. Therefore, concerns and fears have been expressed regarding potential risks of nanoparticles to the environment, health, and safety (Nel et al. 2006; Schmidt 2009). However, studies determining which physicochemical properties of nanomaterials result in toxicity have been scarce.

Previously, we reported findings (Song et al. 2009) regarding a group of patients who were exposed to polyacrylate spray paint in a poorly ventilated workplace for five to thirteen months. Nanoparticles were associated with this polyacrylate coating. Affected workers suffered mysterious clinical symptoms (pleural effusions, progressive pulmonary fibrosis, and pleural damage) and death. Nanoparticles were found in the patients' pulmonary tissues, bronchoalveolar lavage fluid, and chest effusions, as well as in the raw materials used by these workers. It is inferred that these nanoparticles may be related to the patients' disease, but the chemical composition of the nanoparticles remains unknown. For this reason and the fact that none of the nanoparticles was likely to induce the severe toxic effects reported in animal experiments, some researchers have argued that the disease may have been related to other factors such as gases, as the raw material examined by gas chromatograph–mass spectrometer contained many gases, including butanoic acid, butyl ester, acetic acid, toluene, acetic acid ethenyl ester, and 1-ethylene dioxide. Unfortunately, these patients exhibited none of the signs and symptoms related to these irritant or asphyxiant gases, such as coughing, eye irritation, dizziness/headaches, drowsiness, nausea, or vomiting. Additionally, pulmonary clinicopathology showed a progressive feature even in the absence of continued exposure, a major indication that lessened the probability that the observed symptoms were caused by a gas or gases.

In the present study, examination of the patients' biopsies and chest fluids by transmission electron microscopy (TEM) and energy dispersive x-ray analysis (EDX) permitted the isolation and identification of nanomaterials in biopsies. Also, we report the potential deleterious effects of nanomaterials on human lungs, which have not been previously fully described and reported.

Methods

Transmission Electron Microscopy of Pulmonary Biopsies and Chest Membranes and EDX of Nanoparticles

The formaldehyde-fixed and paraffin-embedded pulmonary tissues and/or pleural membranes, obtained from affected workers in a spray paint facility upon admission to Beijing Chaoyang Hospital, Beijing, China, between January 2007 and April 2008, were used for TEM examination and EDX analysis. Tissue fragments of 1 mm^3 (1 mm $\times$ 1 mm $\times$ 1 mm) were cut with a sharp razor blade from distinct, randomly chosen areas of the paraffin

block and reprocessed as follows. Xylene dewaxing was performed in a 50°C oven for two hours to remove paraffin, and tissues were lightly rehydrated with graded acetone (at 40°C in 100% acetone for one hour; and at room temperature in 90%, 70%, 50%, and 30% acetone for fifteen minutes, respectively). Specimens of the samples were rinsed overnight in 0.1 M phosphate buffer (350 mOsm, pH 7.4); postfixed for two hours in osmium tetroxide (1% osmium tetroxide in 0.125 M sodium cacodylate buffer, 400 mOsm, pH 7.4); rinsed again in 0.1 M phosphate buffer (three × ten minutes); passed through stepwise dehydration in increasing concentrations of ethanol (50%, 70%, 90%, and 100%); rinsed with 100% propylene oxide (two × ten minutes); and embedded in Araldite (at 37°C for two hours, 45°C for twelve hours, and 60°C for twenty-four hours). Then they were cut into ultrathin sections (500–800 Å) and stained with uranyl acetate and lead citrate. The samples were then examined at an accelerating voltage of 60 or 200 kV using different TEMs and also analyzed using EDXs (JEOL JEM-2010F, EDX: INCA-IET200 B[5]~U[92]; TECNAI G2 20 S-TWIN, EDX: GENESIS 2000) by different laboratories. Also, changes in cell morphology of lung tissue samples were observed and assessed. The specimen from a lung tumor patient was used as a control in TEM and EDX analysis and was processed as described above.

Analysis of Patients' Pleural Fluids

Nanoparticle Morphology, Size, and Chemical Composition—Pleural effusions were obtained from four of seven patients upon admission to our hospital in April 2008 and were stored at −20°C. Samples were randomly used and melted under normal room conditions. When the chest fluid samples were centrifuged at $123.6 \times g$, stained with uranyl acetate, and air dried, round nanoparticles were observed to be wrapped in a fibrous structure (Song et al. 2009). Thus, at this time, chest effusions were then centrifuged at $8,500 \times g$ at room temperature for ten minutes, and a drop of the resulting supernatant liquid was overlaid onto 400-mesh carbon-coated copper grids (not stained by uranyl acetate), air-dried, and observed using TEM by different laboratories. These preparations were also analyzed by EDX single-spot analysis to illuminate particle morphologies and to identify the particle composition. In addition, qualitative analysis was also performed.

Analysis by Inductively Coupled Plasma Mass Spectrometry (DRC-II, Perkin-Elmer) or Atomic Absorption Flame Spectrophotometry (AA-6800/F, Shimadzu) for Determining Ca, Mg, Cu, Fe, and Zn Concentrations—Chest fluid from three of seven patients was analyzed for Si, Ca, Mg, Cu, Fe, and Zn, since metallic compounds are usually used as additives in coatings production. Chest fluid from patients with lymphoma, lung cancer, or malignant melanoma in our tumor department was used as controls. Certified standard samples of Si, Ca, Mg, Cu, Fe, and Zn were obtained from the National Research Center for Certified Reference Materials, China.

Histological Changes in Patients' Lungs

All examinations were approved by our hospital's ethics commission, and informed consent was obtained before all the examinations and procedures. The biosamples from seven patients included tunica mucosa bronchiorum, pulmonary tissues, and pleural membranes. All of these samples were obtained from patients between January 2007 and April 2008, when the patients were admitted to our hospital and underwent a variety of procedures,

including bronchoscopic examinations with bronchoalveolar lavage and transbronchial lung biopsy, internal thoracoscopic examinations with lung biopsy, and video-assisted thoracic surgery with wedge resection. Pathological changes were carefully observed and revised under light microscopy in different laboratories.

Results

Nanoparticles Observed and Identified in Lung Tissue and Lung Injury under TEM

Early Stage Location of Nanoparticles in Exposed Lungs—In the early stages (within three months of disease onset), nanoparticles 20–21 nm in diameter were observed and found to be located in the cytoplasm (Figure 1A), nuclei and organelles of macrophages, pulmonary microvessels (Figures 1B and 1C), pulmonary vascular endothelial cells, and microlymphatic vessels. In contrast, only a few were observed in alveolar epithelial cells and interstitial tissues. When analyzed by EDX, all of these nanoparticles contained Si, O, P, and S (Figure 1D), and, occasionally, K and Fe were detected. On the other hand, using TEM, the specimen from the control tumor patient was also observed to contain structures resembling nanoparticles (Figure 1E). However, no Si was detected by EDX analysis, but O, S, Cl, and elements from stains were detected (Figure 1F), indicating that these structures were just stains or other cellular components such as glucogen. From comparison with control peaks (peaks of C and Cu oriented on carbon Cu-grids), it was concluded that these were silica nanoparticles. These particles consisted of 20–21 nm primary nanoparticles and agglomerates of these particles, indicating they were engineered nanomaterials. Further qualitative analysis showed that the O/Si ratios at the k atomic orbital varied from 4.43:1 to 18.0:1 by weight-%, and the O relative contents were more than in the O/Si ratio of 1.2–1.6:1, which may have been because there were hydroxyls or H_2O on the silica nanoparticle surfaces, or because of the contribution of O in alveolar cells. In general, particles larger than 100 nm, or other kinds of particles such as nanosilicates, were not observed in patients' lung tissues.

Early Stage Lung Damage in Affected Workers—Pulmonary tissue and cells were found to be deteriorated. Early in the disease process, TEM examination of lung tissue demonstrated hyperplasia and degeneration of type II pneumocytes with short microvilli thinning and loss, and thickening of the basement membrane of type I alveolar epithelial cells, as well as pulmonary interstitial edema. Also, vascular endothelial cell damage was noted with the swelling and vacuolization of cell organelles and the thickening of the basement membrane. The blood–gas barrier appeared fuzzy and was much thicker than normal (>0.5 μm), and its structure was difficult to distinguish (Figure 1B).

Late-Stage Location of Nanoparticles in Exposed Lungs—In the late disease stage (eighteen months, just prior to death), few nanoparticles were observed in pulmonary cells and interstitial tissue, as well a few in macrophages. However, some fibrous nanostructured bodies ~70 nm in length were observed in the nuclei and cytoplasm of alveolar epithelial cells, where they formed tangled agglomerates (Figure 2A) or crossed the nuclear membrane of alveolar epithelial cells. Using EDX single spot analysis, these fibrous nanostructured bodies were found to contain Fe, Ca, and Mg, but not Si. Also, microscale particles were not

observed in the patient's lung tissues, which suggested that microscale particles may be less likely to be involved in the lung injury process.

Late-Stage Lung Damage in Affected Workers—In late-stage disease, damage to pulmonary tissue was more prominent than that in the early stage. Hyperplasia and vacuolar degeneration of type II pneumocytes with thinning and loss of surface microvilli (Figure 2B), as well as thickening and blurring of type I epithelial basement membranes and vascular endothelial cell basement membranes, was observed. Also, the blood–gas barrier structure appeared fuzzy and difficult to distinguish. Red blood cells were observed in alveolar spaces, which is indicative of potential alveolar hemorrhage and edema. Pulmonary fibrosis with fibroblast proliferation and fibrinous necrosis was also noted, and under TEM, pleural membranes showed edema, fibrosis, looseness, and blurring of cell structures. These observations were consistent with the present diagnosis of pulmonary pathology. Also, a great number of macrophages were observed as aggregations in the late stage as in the early disease process, indicating that macrophages may play some roles in the development of the disease; these particle-laden aggregations were ever seen in pulmonary illness caused by microscale silica (Kim et al. 2001).

Morphology and Size of Chest Fluid Nanoparticles

Particles with different sizes varying from ~20 nm to ~2 nm in diameter were observed (Figure 3A) in patients' pleural effusions, although homogeneous nanoparticles were noted when pleural effusions were centrifuged at $123.6 \times g$ (Song et al. 2009). When analyzed by EDX, the particles contained Si, O, C, and Cu (Figure 3B). By comparison with a blank (Figure 3C), these particles were identified as silica nanoparticles (where C and Cu peaks originated from the carbon-coated copper grids). Further qualitative analysis showed that the O/Si ratio varied from 3.98:1 to 7.75:1 by atomic mass-% and from 2.28:1 to 4.34:1 by weight-%, which suggests the presence of hydroxyls or H_2O on the silica nanoparticle surfaces. However, the sizes of the silica nanoparticles in the pleural effusions were a little smaller than in the pulmonary tissue, possibly because of a size-dependent translocation of particles from the lungs.

Importantly, in one patient's pleural effusions, layered crystals and cleavage fragments, varying in size from micro- to nanoscale, were noted (Figure 3D). Some crystals contained Si, Ca, Mg, S, Cl, and O, indicating the presence of a magnesium silicate such as talc, and some contained more complex mixtures of Si, Ca, Mg, Al, P, S, Cl, and O (Figure 3E). Additionally, nanosilica particles, as well as nanosilicate particles containing Si, Ca, Mg, Al, K, Na, Ba, P, S, Cl, and O, were confirmed by EDX analysis and noted to be scattered around the microsilicates. Si was detected in every particle observed in the pleural effusions, but with varying relative contents.

In summary, we conducted EDX analysis of four patients' (out of seven) pleural effusions and/or their lung biopsies in different laboratories. These four patients included the nineteen-year-old and the twenty-nine-year-old female patients who died of pulmonary failure, and the eighteen-year-old and the forty-seven-year-old female patients who were severely disabled (EDX analysis was not conducted in the other female patients because of a lack of

biosamples). We found that silica nanoparticles existed in all four patients, either in pulmonary biopsies (early stage) or pleural effusions. Occasionally, nano- and microscale silicates were found in chest fluids, but not in any of the four patients' lung tissues. The TEM images presented here indicate that these silica nanoparticles identified—the highly spherical and uniform nanoscale particles—are most likely amorphous in nature, as is the case for most known engineered forms of spherical silica in the nanoscale size range.

Inductively Coupled Plasma Mass Spectrometry and Atomic Absorption Flame Spectrophotometry of Pleural Effusions

Concentrations of Ca, Mg, Cu, Fe, and Zn were analyzed in chest fluids, showing that the concentrations of these elements were lower in the patients' pleural effusions than in the tumor patient controls (effusion, control', $n = 3$): Cu, 0.282 ± 0.216 mg/L; Cu', 0.721 ± 0.091 mg/L; Mg, 8.190 ± 4.609 mg/L; Mg', 17.623 ± 1.753 mg/L; Ca, 17.423 ± 10.782 mg/L; Ca', 81.694 ± 9.779 mg/L; Fe, 0.310 ± 0.208 mg/L; Fe', 3.888 ± 4.813 mg/L; Zn, 0.125 ± 0.128 mg/L; and Zn', 0.363 ± 0.216 mg/L. However, the concentration of Si in patients' pleural effusions was 4.844 ± 0.431 mg/L, about two times of that in tumor patients' chest fluids (2.530 ± 0.206 mg/L).

Histological Changes in Patients' Lungs

In the early disease stage, pathological examination using light microscopy showed the effusion of inflammatory cells in tunica mucosa bronchiorum; aggregations of macrophages and inflammatory cells; proteinaceous effusions in the alveolar space; swollen and widened alveolar septa with scattered neutrophil leukocytes; and pulmonary fibrosis (Figure 4A). Pathological study of pleura exhibited fibrinous and inflammatory cells, foreign-body granulomas, and hemorrhage. The results of all patients were consistent but nonspecific.

In the late stage, damage to pulmonary tissue was similar to but more prominent than that in the early stage. Pulmonary alveoli were partly emphysematous, with aggregations of macrophages and type II alveolar epithelial cell proliferations, and the alveolar septum was widened with blood vessel dilatation and congestion (Figure 4B). Pathological study on pleura showed fibrous thickening and swelling of the pleural membrane, fibroblast proliferation, lymphocyte aggregation, and nodulus lymphaticus formation.

Discussion

From the above observations and analyses, silica nanoparticles were identified in patients' lungs and their pleural effusions. Distribution and translocation of these nanoparticles were determined mainly in pulmonary microvessels, vascular endothelial cells, macrophages, and microlymphatic vessels of patients' lungs. A few particles were found in alveolar epithelial cells and pulmonary interstitial tissue (with no microscale particles present). In pleural effusions, the particles appeared slightly smaller in size than those in lung tissues, and micro- and nanosilicates were noted in one patient's chest effusion and contained thirteen to fifteen different elements and widely varying O/Si ratios. Notably, damage to vascular endothelial cells, alveolar epithelial cells, and macrophages, as well as the blood–gas barrier, was observed. Additionally, the concentration of Si in patients' pleural effusions was about

two times that in tumor patients' chest fluids. These data provided important information to understand the unique nanoparticle-induced lung disease process, which seems to be dependent on where the nanoparticles are located and whether they are persistent in the lung.

The toxicity of silica has been widely studied because of its ubiquity and wide use in many industries. Exposure to silica (mainly crystalline silica) can result in or contribute to a series of severe respiratory diseases, including silicosis, interstitial fibrosis, industrial bronchitis, small airway disease, emphysema, and vascular diseases, as well as immunologic reactions (Ding et al. 2002; Hnizdo and Vallyathan, 2003; Merget et al. 2002; Thibodeau et al. 2004). Even though amorphous silica appears less toxic than the crystalline form, toxicological studies of amorphous silica nanoparticles have shown that amorphous silica increases reactive oxygen species concentrations, reduces glutathione levels, and induces pro-inflammatory, inflammatory, and oxidative stress responses both in vivo and in vitro (Kaewamatawong et al. 2006; Park and Park 2009; Slowing et al. 2009; Wang et al. 2009; Ye et al. 2010). One of the notable bio-effects of amorphous silica nanoparticles is that they can enter cell nuclei (Chen and von Mikecz 2005), including human lung cells (Song et al. 2009), where they reduce aberrant clusters of topoisomerase I and protein aggregates in the nucleoplasm. In vitro studies also show that amorphous silica nanoparticles disturb mitochondrial function and lower cell survival by decreasing cell survival signaling in human neural cells (Lai et al. 2010), and they exert cytotoxicities by altering protein expression in HaCaT cells (Yang et al. 2010). A recent study found that amorphous silica nanoparticles (70 nm) localize in the cytoplasm, nucleus, and mitochondria in mouse liver, and they induce mutagenic activity in vitro (Nabeshi et al. 2011). Moreover, amorphous nanosilica has been shown to accumulate in the lung, liver, kidney, gut, bone marrow, and brain in animal experiments and cause multiorgan damage (Kaewamatawong et al. 2006; Nishimori et al. 2009a; Nishimori et al. 2009b; Oberdörster et al. 2005).

Our present findings that silica nanoparticles localized in cytoplasm, subcellular organelles, and cell nuclei, entered pulmonary microvessels, and thereby reached extrapulmonary multiorgans through systemic circulation raise important concerns: (1) Did these silica nanoparticles in the nuclei potentially bind to the DNA phosphate backbone, influence nuclear integrity, and trigger genotoxicity by physical interaction, forming intranuclear protein aggregates, and regulating redox-sensitive transcription factors and DNA-damage responsive signaling, as seen in animal-based nanotoxicological studies (Chen and von Mikecz 2005; Nabeshi et al. 2011; Singh et al. 2009)? (2) Did these silica nanoparticles in cytoplasm exert cytotoxicity by increasing reactive oxygen species and by inducing pro-inflammatory, inflammatory, and oxidative stress responses, as seen both in vivo and in vitro (Kaewamatawong et al. 2006; Park and Park 2009; Slowing et al. 2009; Ye et al. 2010)? (3) Did these silica nanoparticles enter extrapulmonary organs through systemic circulation and cause multiorgan damage, as seen in animal experiments (Kaewamatawong et al. 2006; Nishimori et al. 2009a; Nishimori et al. 2009b; Oberdörster et al. 2005)? All of the above concerns highlight the urgent need and the importance of the safe usage and risk assessment of nanomaterials, and of developing prevention strategies.

Given the well-documented toxicity of microscale silica in humans and findings of amorphous silica nanoparticles in animals (Kaewamatawong et al. 2006; Nishimori et al.

2009a; Nishimori et al. 2009b; Oberdörster et al. 2005), it is possible that these silica nanoparticles may have contributed in part to these patients' disease, whether they exerted toxicities directly or acted as carriers, although further evidence is needed to make a direct causal linkage between the silica nanoparticles in patients' lungs and their respiratory problems and the death of two workers as they worked under complex conditions and inhaled a cocktail of toxic materials. To date, little information regarding the clinical toxicity of nanosilica has been published. As nano- and microscale silica are found to induce cytokine release and apoptosis in macrophages in in vitro and in vivo studies (Ding et al. 2002; Park and Park 2009; Thibodeau et al. 2004; Wang et al. 2009; Ye et al. 2010), taken together with our findings of nanosilica in macrophages undergoing apoptosis (Song et al. 2009), it is suggested here that apoptosis is one mechanism of nanosilica-related macrophage damage in humans. Also, in these patients, the clinical manifestation of nonspecific inflammation detected in CT scans and pathological examinations may have been partly caused by silica nanoparticle accumulation and the resulting induced inflammatory response.

In pulmonary illness caused by microscale silica, macrophages have been observed as particle-laden aggregations (Kim et al. 2001), a reaction that is typically seen with inert dusts. Similar aggregations of macrophages were observed in our patients in the early stage of disease, with numerous silica nanoparticles aggregating in the cytoplasm, mitochondria, lysosomes, and karyoplasm of macrophages. The retention half-life of solid particles in the alveolar region, mediated by alveolar macrophages through phagocytosis of deposited particles, is about 70 days in rats and up to 700 days in humans (Oberdörster et al. 2005). In our patients, the retention half-life of silica nanoparticles appeared to be about 100 days, as about eighteen months later following the final raw material exposure, few nanoparticles were observed in pulmonary cells and interstitial tissue, as well a few in macrophages, which is consistent with previous literature reporting that the retention half-life of nanoparticles by the mechanical alveolar macrophage-mediated clearance is about 70 days (Hoet et al. 2004).

The reported patients had been exposed to polyacrylate coatings, which usually have several components of binders, pigments, solvents, fillers, and additives (Liu 2008). Fillers and additives are generally composed of natural or synthetic minerals, such as silicon dioxide, barium sulfate, calcium carbonate, silicates (talc, mica, or kaolinite), or a complex mixture of the above materials, to produce special and improved functions, such as water resistance, transparency, and flame retardation (Liu 2008; Wang et al. 2006; Zhou et al. 2002). Because of their small size, large specific surface area, and alkyl groups in different bonding states, silica nanoparticles in coatings can markedly improve the suspension stability, weatherability, tensile strength, and resistance of a coating to washing, infrared irradiation, abrasion, and heat while maintaining a clear surface (Wang et al. 2006; Zhou et al. 2002). In contrast, microsilica can increase only the hardness and abrasion resistance (Zhou et al. 2002). Similarly, layered silicates, another very popular coating ingredient, play an important role as adsorbents, catalysts, and ionic exchangers in the production of nanocoatings and can greatly increase thermal stability and act as fire retardants in the form of nanocomposites (Alexandre and Dubois 2000; Schmidt and Giannelis 2010).

Given the benefits of nanosilica and/or nanosilicates, they are sometimes used concurrently in varying ratios to each other in the production of nanocomposite coatings (Liu 2008) to obtain specific coating characteristics. Thus, a possible rough sketch can be made of the coatings used at these patients' workplace: filters and additives of nanosilica and/or micro- and nanosilicates, a film-forming polyacrylate agent, and various solvents, including butanoic acid, acetic acid, and toluene. Furthermore, using inductively coupled plasma atomic emission spectrometry examination (Ma 2009), the powder in the raw materials used in the workplace (the spray painting) was found to contain these elements in the following percentages: Si, 0.016; Ca, 0.20; Mg, 0.051; K, 0.015; Na, 0.82; Ba, 0.069; P, 0.048; Cu, 0.0090; Fe, 0.098; and Zn, 0.0085. These results are almost identical to our findings of silica nanoparticles and micro- and nanosilicates in patients' pleural effusions that contain Si, Ca, Mg, K, Na, Ba, Al, P, S, Cl, and O. When coatings were sprayed, heated, and dried in the workplace, these nanosilica and/or nanosilicates in the coatings were possibly present in the air as floccule; entered the pulmonary alveoli, blood, and lymph systems; and finally reached extrapulmonary organs of the patients, as observed in animal experiments (Nishimori et al. 2009a; Oberdörster et al. 2005; Oberdörster 2010; Singh et al. 2009). Thus they potentially contributed in part to the multiorgan injuries seen in our patients (Song et al. 2009).

Another important material found in one patient was micro- and nanosilicates. It appears a little puzzling that the micro- and nanosilicates were noted in one patient's chest effusion, since only nanoparticles but not microscale particles were observed in the raw materials used in the workplace. Also, what were the fibrous nanostructured bodies in alveolar epithelial cells, and how did they get there? The reason may be the raw materials—a poor-quality product (a "three-no" product: no trademark, origin, or material safety data sheet, chosen to decrease expenses)—used in the workers' polystyrene processing surroundings. Another reason is that, in reality, workers are usually exposed to very complex conditions in which nanomaterials with different sizes, shapes, and chemical composition may be present and there is also the possible presence of microscale materials and some gases, which could potentially contribute to causing severe damage.

The sizes of silica nanoparticles in pleural effusions were not identical to those in alveolar tissue, but a little smaller, possibly a result of the size-selective differences in particle immobilization in lungs. Typically, the smaller the nanoparticles, the deeper they can travel into the lung, as reviewed in several articles (Borm et al. 2006; Hoet et al. 2004; Oberdörster et al. 2005). This particle size–dependent organ distribution has been confirmed in properties of iridium-192–radiolabeled nanoparticles (Semmler-Behnke et al. 2007) and gold nanoparticles (Sadauskas et al. 2009). Another reason is probably the chest fluid sampling, as homogeneous nanoparticles were noted when pleural effusions were centrifuged at $123.6 \times g$ (Song et al. 2009).

There are still many outstanding questions here. For example, what is the possible surface contamination of silica nanoparticles? In proper perspective, however, these questions are not as important or urgent as questions regarding how to prevent the potential risks of these nanomaterials to workers and the environment.

Our present study shows that silica nanoparticles can arrive at workers' lungs, chest effusions, and pulmonary circulation, and they may have contributed in part to the workers' illness and death, highlighting the urgent need for safety protocols that protect workers. Protocols or solutions may include regulations for occupational health and safety in nanofield work or research; workplace exposure assessment, monitoring, and controls; medical prescreening and surveillance; establishing industrial hygiene guidelines; and effective personal protective equipment or application of appropriate safeguards. In addition, given the severity of the disease as seen in our patients, and the great difficulties in diagnosis and treatment, it is a new challenge for our clinical doctors in terms of how to prevent, diagnose, and treat the disease or injury. Thus far, no medical laboratories in China are equipped with TEM and analytic systems such as EDX, x-ray diffraction, or x-ray photoelectron spectrometry, and the few top materials science and engineering institutes, which are well equipped, have staff that usually lack the proper biomedical knowledge and maintain TEM configurations unsuitable for biological samples. Most importantly, some patients exposed or suspected to have been exposed to nanomaterials are found with unusual clinical manifestations, making it very difficult to determine a causal relation between their nanomaterials exposure and their disorders.

In conclusion, our findings of nanosilica in patients' biopsies and pleural effusions, together with our previous report (Song et al. 2009), present a clue that these silica nanoparticles may have contributed in part to the illness reported in these workers. Our findings highlight the urgent need and the importance of the nanosafety study, as well as the urgent need for safety protocols that protect workers and the environment. Our data in humans may provide useful information for intensely increased nanotoxicology research that would mimic nanomaterial exposure using animals or in vitro models to determine mechanisms. Nanomaterials offer great benefits as well as potential risks, which raises the question of how to enjoy their benefits while minimizing related potential hazards to humans as well as the environment. Answering these questions is an urgent and difficult global-level task.

Acknowledgments

Abbreviations

BALF   bronchoalveolar lavage fluid

EDX   energy dispersive x-ray analysis

TBLB   transbronchial lung biopsy

TEM   transmission electron microscopy

VATS   video-assisted thoracic surgery

References

Alexandre M, Dubois P. Polymer-layered silicate nanocomposites: Preparation, properties and uses of a new class of materials. Mater Sci Eng. 2000; 28:1–63.

Borm PJ, Robbins D, Haubold S, Kuhlbusch T, Fissan H, Donaldson K, Schins R, Stone V, Kreyling W, Lademann J, Krutmann J, Warheit D, Oberdörster E. The potential risks of nanomaterials: A review carried out for ECETOC. Part Fibre Toxicol. 2006; 3:11. [PubMed: 16907977]

Chen M, von Mikecz A. Formation of nucleoplasmic protein aggregates impairs nuclear function in response to SiO$_2$ nanoparticles. Exp Cell Res. 2005; 305:51–62. [PubMed: 15777787]

Ding M, Chen F, Shi X, Yucesoy B, Mossman B, Vallyathan V. Diseases caused by silica: Mechanisms of injury and disease development. Int Immunopharmacol. 2002; 2:173–82. [PubMed: 11811922]

Hnizdo E, Vallyathan V. Chronic obstructive pulmonary disease due to occupational exposure to silica dust: A review of epidemiological and pathological evidence. Occup Environ Med. 2003; 60:237–43. [PubMed: 12660371]

Hoet PH, Brüske-Hohlfeld I, Salata OV. Nanoparticles — known and unknown health risks. J Nanobiotechnology. 2004; 2:12. [PubMed: 15588280]

Kaewamatawong T, Shimada A, Okajima M, Inoue H, Morita T, Inoue K, Takano H. Acute and subacute pulmonary toxicity of low dose of ultrafine colloidal silica particles in mice after intratracheal instillation. Toxicol Pathol. 2006; 34:958–65. [PubMed: 17178696]

Kim KI, Kim CW, Lee MK, Lee KS, Park CK, Choi SJ, Kim JG. Imaging of occupational lung disease. Radiographics. 2001; 21:1371–91. [PubMed: 11706211]

Lai JC, Ananthakrishnan G, Jandhyam S, Dukhande VV, Bhushan A, Gokhale M, Daniels CK, Leung SW. Treatment of human astrocytoma U87 cells with silicon dioxide nanoparticles lowers their survival and alters their expression of mitochondrial and cell signaling proteins. Int J Nanomedicine. 2010; 5:715–23. [PubMed: 21042417]

Liu, GJ. Chem Ind Press (CIP) (Beijng). 1st. 2008. Nanomaterials and modified coatings; p. 150-70.

Lux report. Nanomaterials State of the Market Q3 2008: Stealth Success, Broad Impact. 2008. https://portal.luxresearchinc.com/research/document_excerpt/3735

Ma, ZF. Master's Thesis. Tangshan, China: Hebei United University; 2009. A virulence study for organic polymer A causing lung tissue damage in rats.

Merget R, Bauer T, Kupper H, Philippou S, Bauer H, Breitstadt R, Bruening T. Health hazards due to the inhalation of amorphous silica. Arch Toxicol. 2002; 75:625–34. [PubMed: 11876495]

Nabeshi H, Yoshikawa T, Matsuyama K, Nakazato Y, Matsuo K, Arimori A, Isobe M, Tochigi S, Kondoh S, Hirai T, Akase T, Yamashita T, Yamashita K, Yoshida T, Nagano K, Abe Y, Yoshioka Y, Kamada H, Imazawa T, Itoh N, Nakagawa S, Mayumi T, Tsunoda SI, Tsutsumi Y. Systemic distribution, nuclear entry and cytotoxicity of amorphous nanosilica following topical application. Biomaterials. 2011; 32:2713–24. [PubMed: 21262533]

Nel A, Xia T, Madler L, Li N. Toxic potential of materials at the nanolevel. Science. 2006; 311:622–27. [PubMed: 16456071]

Nishimori H, Kondoh M, Isoda K, Tsunoda S, Tsutsumi Y, Yagi K. Histological analysis of 70-nm silica particles-induced chronic toxicity in mice. Eur J Pharm Biopharm. 2009a; 72:626–29. [PubMed: 19341796]

Nishimori H, Kondoh M, Isoda K, Tsunoda S, Tsutsumi Y, Yagi K. Silica nanoparticles as hepatotoxicants. Eur J Pharm Biopharm. 2009b; 72:496–501. [PubMed: 19232391]

Oberdörster G. Safety assessment for nanotechnology and nanomedicine: concepts of nanotoxicology. J Intern Med. 2010; 267:89–105. [PubMed: 20059646]

Oberdörster G, Oberdörster E, Oberdörster J. Nanotoxicology: An emerging discipline evolving from studies of ultrafine particles. Environ Health Perspect. 2005; 113:823–39. [PubMed: 16002369]

Park EJ, Park K. Oxidative stress and pro-inflammatory responses induced by silica nanoparticles in vivo and in vitro. Toxicol Lett. 2009; 184:18–25. [PubMed: 19022359]

Sadauskas E, Jacobsen NR, Danscher G, Stoltenberg M, Vogel U, Larsen A, Kreyling W, Wallin H. Biodistribution of gold nanoparticles in mouse lung following intratracheal instillation. Chem Cent J. 2009; 3:16. [PubMed: 19930546]

Schmidt CW. Nanotechnology-related environment, health, and safety research: Examining the national strategy. Environ Health Perspect. 2009; 117:A158–61. [PubMed: 19440480]

Schmidt DF, Giannelis EP. Silicate dispersion and mechanical reinforcement in polysiloxane / layered silicate nanocomposites. Chem Mater. 2010; 22:167–74.

Semmler-Behnke M, Takenaka S, Fertsch S, Wenk A, Seitz J, Mayer P, Oberdörster G, Kreyling WG. Efficient elimination of inhaled nanoparticles from the alveolar region: Evidence for interstitial uptake and subsequent reentrainment onto airways epithelium. Environ Health Perspect. 2007; 115:728–33. [PubMed: 17520060]

Singh N, Manshian B, Jenkins GJ, Griffiths SM, Williams PM, Maffeis TG, Wright CJ, Doak SH. NanoGenotoxicology: The DNA damaging potential of engineered nanomaterials. Biomaterials. 2009; 30:3891–914. [PubMed: 19427031]

Slowing II, Wu CW, Vivero-Escoto JL, Lin VSY. Mesoporous silica nanoparticles for reducing hemolytic activity toward mammalian red blood cells. Small. 2009; 5:57–62. [PubMed: 19051185]

Song Y, Li X, Du X. Exposure to nanoparticles is related to pleural effusion, pulmonary fibrosis and granuloma. Eur Respir J. 2009; 34:559–67. [PubMed: 19696157]

Thibodeau MS, Giardina C, Knecht DA, Helble J, Hubbard AK. Silica-induced apoptosis in mouse alveolar macrophages is initiated by lysosomal enzyme activity. Toxicol Sci. 2004; 80:34–48. [PubMed: 15056807]

Wang F, Gao F, Lan M, Yuan H, Huang Y, Liu J. Oxidative stress contributes to silica nanoparticle-induced cytotoxicity in human embryonic kidney cells. Toxicol In Vitro. 2009; 23:808–15. [PubMed: 19401228]

Wang Z, Han E, Ke W. An investigation into fire protection and water resistance of intumescent nano-coatings. Surf Coat Technol. 2006; 201:1528–35.

Yang X, Liu J, He H, Zhou L, Gong C, Wang X, Yang L, Yuan J, Huang H, He L, Zhang B, Zhuang Z. SiO_2 nanoparticles induce cytotoxicity and protein expression alteration in HaCaT cells. Part Fibre Toxicol. 2010; 19:7.

Ye Y, Liu J, Xu J, Sun L, Chen M, Lan M. Nano-SiO_2 induces apoptosis via activation of p53 and Bax mediated by oxidative stress in human hepatic cell line. Toxicol In Vitro. 2010; 24:751–58. [PubMed: 20060462]

Zhou S, Wu L, Sun J, Shen W. The change of the properties of acrylic-based polyurethane via addition of nano-silica. Prog Org Coat. 2002; 45:33–42.
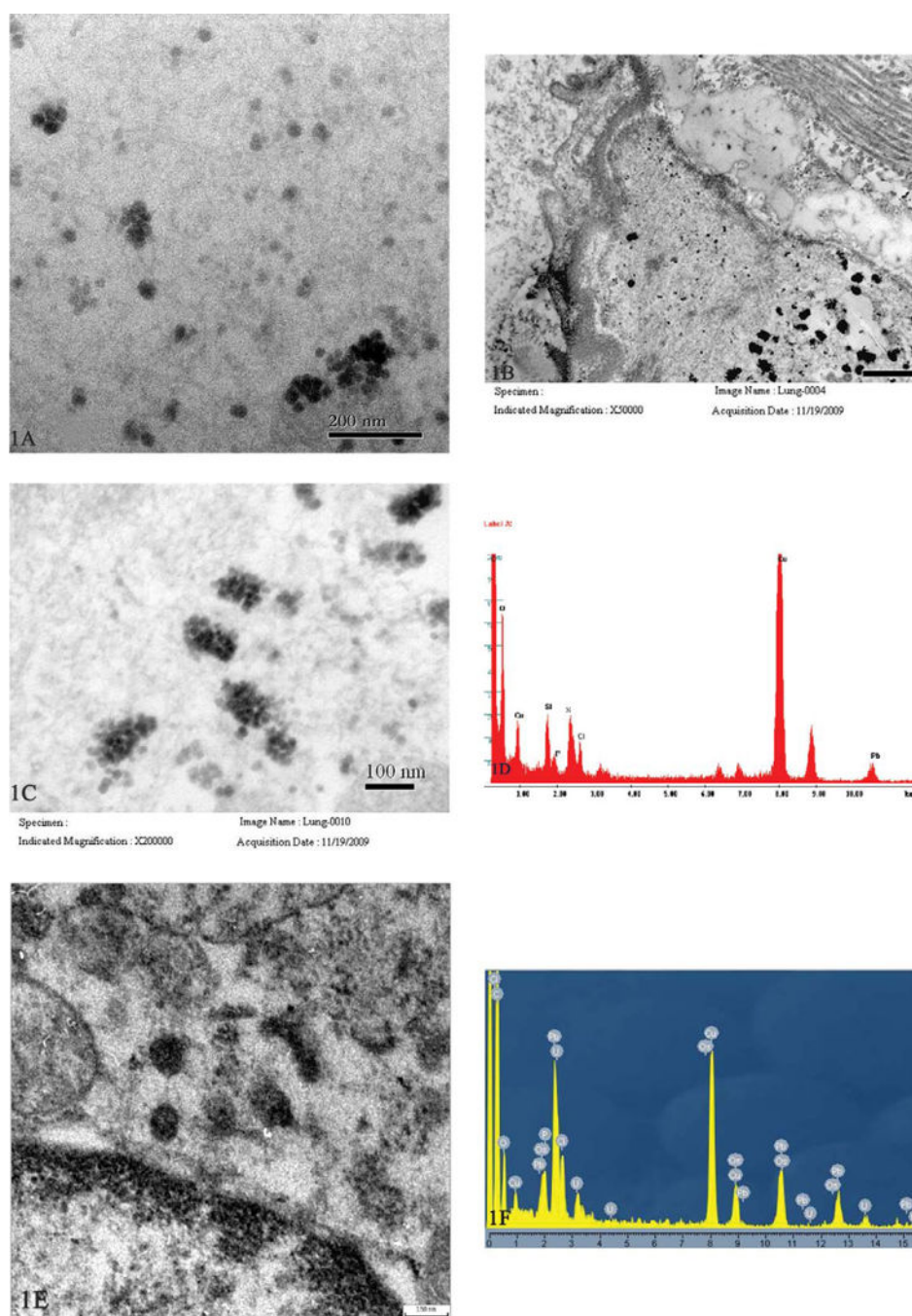
Figure 1.
Transmission electron microscopy images of silica nanoparticles obtained from lung tissues of a nineteen-year-old female worker who was severely disabled. Nanoparticles 20–21 nm in diameter scattered in cytoplasm of a macrophage (A, scale bar = 200 nm), and a pulmonary microvessel (B, scale bar = 500 nm; and C, scale bar = 100 nm). Energy dispersive x-ray analysis (TECNAI G2 20 S-TWIN, EDX: GENESIS 2000) revealed they were silica nanoparticles (D), peaks of C and Cu oriented on carbon Cu-grids, and Pb from stains. Structures resembling nanoparticles were also observed in the specimen from the control

tumor patient (E, scale bar = 150 nm). No Si was detected, but there were stains (F) (JEOL JEM-2010F, EDX: INCA-IET200 $B^5 \sim U^{92}$).
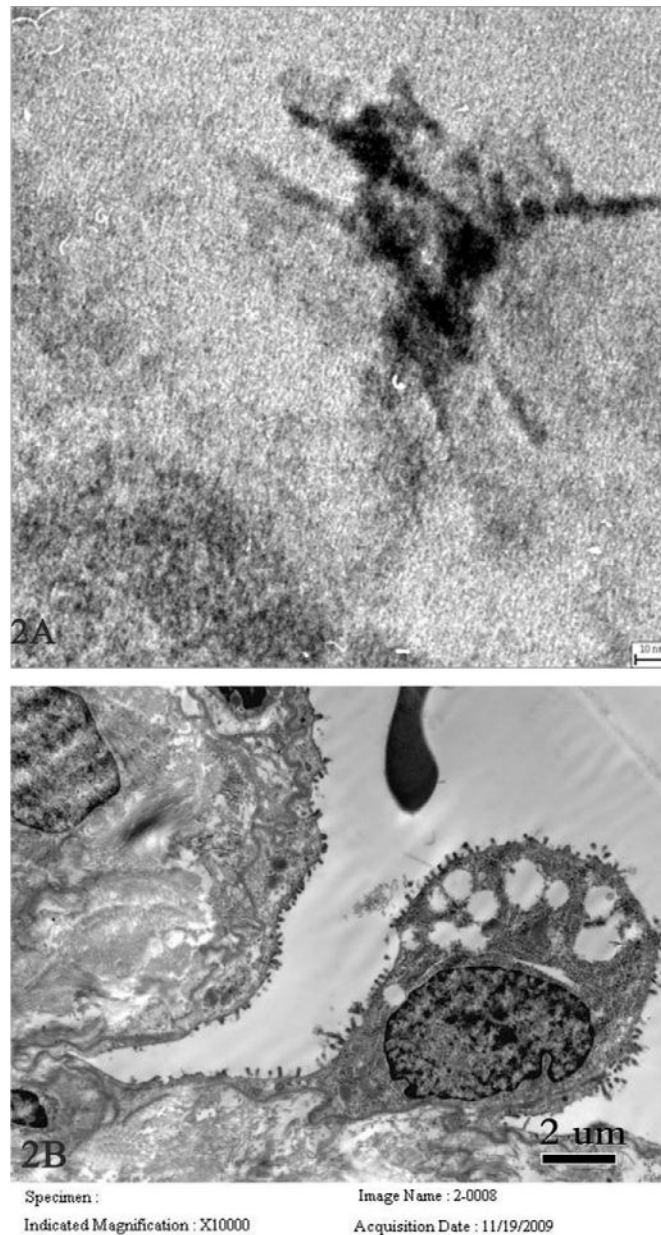
Figure 2.
Transmission electron microscopy images of fibrous nanostructured bodies and pulmonary damage in another nineteen-year-old female worker who died eighteen months after symptom onset. Fibrous nanostructured bodies ~70 nm in length were observed in the nuclei of an alveolar epithelial cell, where the nanostructure is in tangled form (A, scale bar = 30 nm). B (scale bar = 2 μm) shows a fraction of a red blood cell in alveolar spaces, hyperplasia, and vacuolar degeneration of type II pneumocytes with thinning and loss of surface microvilli.
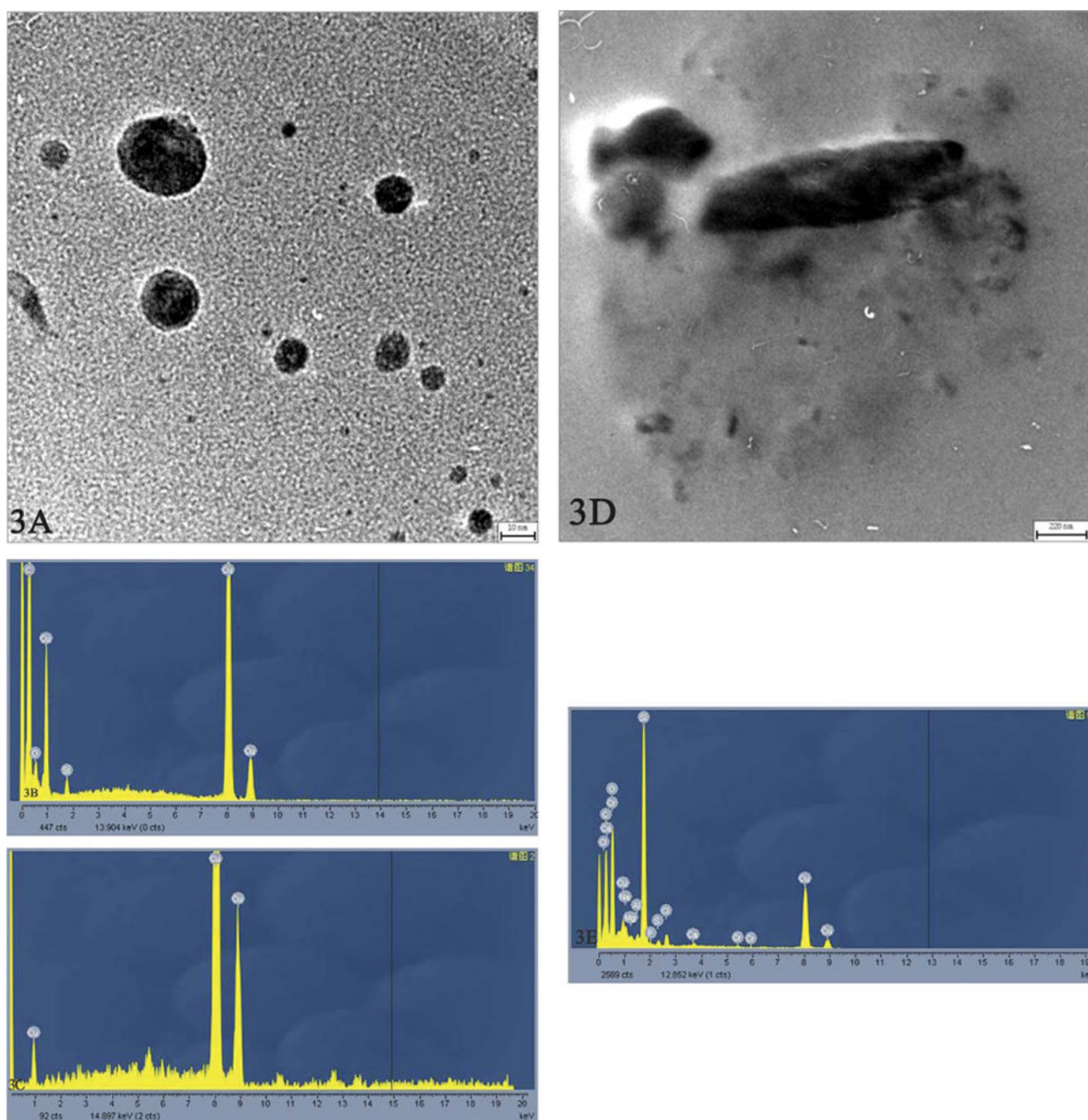
Figure 3.
Transmission electron microscopy images of nanomaterials obtained from chest fluid in a twenty-nine-year-old female worker who died twenty-one months after symptom onset. Nanoparticles varying from ~20 nm to ~2 nm in diameter were observed (A, scale bar = 10 nm). Energy dispersive x-ray analysis (TECNAI G2 20 S-TWIN, EDX: GENESIS 2000) revealed that they were silica nanoparticles (B, C). Layered crystals with their cleavage fragments were noted, varying from nano- to microscale in size (D, scale bar = 220 nm) and containing the more complex elements of Si, Ca, Mg, Al, Cr, P, S, Cl, and O (E).
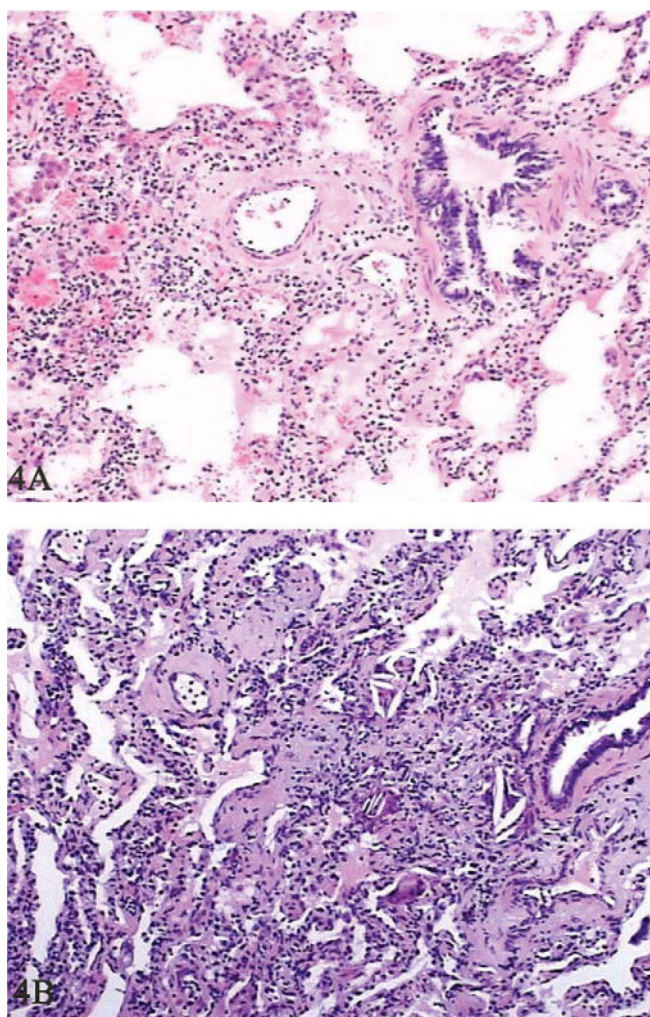
Figure 4.
Histological changes in patients' lungs. In the early stage, aggregation of macrophages in the alveolar space, swollen and widened alveolar septa, and pulmonary fibrosis were observed (A, hematoxylin and eosin stain, 100×). In the later disease process, pulmonary alveoli were partly emphysematous with aggregations of macrophages and proliferations of type II alveolar epithelial cells, and the alveolar septum was widened with blood vessel dilatation and congestion (B, hematoxylin and eosin, 100×).